Counterion condensation on charged micelles in an aqueous electrolyte solution as studied with combined small-angle neutron scattering and small-angle x-ray scattering

2006 J. Phys.: Condens. Matter 18 11399

(http://iopscience.iop.org/0953-8984/18/50/001)

INSTITUTE OF PHYSICS PUBLISHING JOURNAL OF PHYSICS: CONDENSED MATTER

J. Phys.: Condens. Matter **18** (2006) 11399–11410 doi:10.1088/0953-8984/18/50/001

Counterion condensation on charged micelles in an aqueous electrolyte solution as studied with combined small-angle neutron scattering and small-angle x-ray scattering

V K Aswal[1], J Kohlbrecher[2], P S Goyal[3], H Amenitsch[4] and S Bernstorff[5]

[1] Solid State Physics Division, Bhabha Atomic Research Centre, Mumbai 400 085, India
[2] Laboratory for Neutron Scattering, ETHZ Zurich & PSI Villigen, CH-5232 Villigen PSI, Switzerland
[3] UGC-DAE Consortium for Scientific Research, Bhabha Atomic Research Centre, Mumbai 400 085, India
[4] Institute of Biophysics and X-ray Structure Research, Austrian Academy of Sciences, Graz A-8010, Austria
[5] Sincrotrone Trieste, Area Science Park, I-34012 Bassovizza, Trieste, Italy

E-mail: vkaswal@barc.gov.in

Received 16 August 2006, in final form 29 September 2006
Published 27 November 2006
Online at stacks.iop.org/JPhysCM/18/11399

Abstract

Combined studies of small-angle neutron scattering and small-angle x-ray scattering have been carried out for the direct observation of counterion condensation on charged micelles of two cationic surfactants, cetyltrimethylammonium bromide (CTABr) and cetyltrimethylammonium chloride (CTACl) in aqueous electrolyte solutions. The addition of the electrolytes KCl and KBr in the CTABr and CTACl micellar solutions, respectively, yields an increase in the counterion condensation as well as the exchange of the counterions. It is found that the counterions in CTABr/KCl and CTACl/KBr micellar solutions are exchanged to the extent of maintaining the same concentration gradient for both the counterions (Br^- and Cl^-) around the charged micelles with respect to the solution.

(Some figures in this article are in colour only in the electronic version)

1. Introduction

Micellar solutions are suspensions of colloidal aggregates of surfactant molecules in aqueous solutions. A surfactant molecule consists of a polar hydrophilic head group and a long hydrophobic chain connected to the head group. The coexistence of the two opposite types of behaviour (hydrophilic and hydrophobic) in the same molecule leads to self-aggregation of the surfactant molecules when dissolved in water. The aggregates are called micelles [1, 2].

Surfactant molecules such as cetyltrimethylammonium bromide (CTABr) ionize in aqueous solution and the corresponding micelles are aggregates of CTA^+ ions. The micelle is charged and the Br^- ions, known as counterions, tend to stay near the CTA^+ micellar surface. The counterions located at short enough distances from the colloidal surface feel a very strong electrostatic attraction compared with the thermal energy k_BT and these counterions are described as bound to or condensed on the colloid. Since the works of Oosawa [3] and Manning [4], the concept of counterion condensation has been widely accepted in the field of linear polyelectrolytes. It has been shown that when the charge density on an infinitely long cylinder is increased beyond a critical value, counterions condense around the cylinder so as to reduce the effective charge density to the critical value. Similar concepts have also been used for colloidal suspensions made of spherical charged colloids [5–7]. In charged micellar solutions, the counterion condensation plays a very important role in deciding the effective charge on the micelle and hence the formation, structure and interaction of the micelles [8–12].

Small-angle scattering covers a length scale where most of the micelle structures starting from spherical to rod-like or disc-like shapes are formed [13]. Small-angle neutron scattering (SANS) and small-angle x-ray scattering (SAXS) studies in combination provide a direct method for studying the counterion condensation on ionic micelles. While neutron scattering in micellar solutions is from the core of the micelle, x-rays are largely scattered by counterions, especially when the counterion has a large atomic number (e.g. Br^-) [14–16]. The neutron scattering intensity from the counterion distribution is negligible in comparison to that from the core. Thus neutrons 'see' the core of the micelle and x-rays give information relating to the counterion condensation around the micelle. In this paper, we show a combined use of SANS and SAXS for the direct observation of counterion condensation on charged micellar solutions of two cationic surfactants CTABr and CTACl in the presence of electrolytes KCl and KBr, respectively.

2. Experiments

Small-angle neutron scattering experiments were carried out using the SANS diffractometer at the Swiss Spallation Neutron Source SINQ, Paul Scherrer Institute, Switzerland [17]. The wavelength of the neutron beam was 4.8 Å and the experiments were performed on two different samples to detector distances of 2 and 8 m to cover a Q range of 0.007–0.30 $Å^{-1}$. Small-angle x-ray scattering experiments were performed at the SAXS beamline of the synchrotron source ELETTRA, Trieste, Italy [18]. The wavelength of the x-ray beam was 1.54 Å (8 keV) and the data were recorded in the Q range of 0.015–0.3 $Å^{-1}$. All the surfactants and electrolytes used were obtained from Fluka. The samples were prepared by dissolving known amounts of surfactants and electrolytes in D_2O. The use of D_2O as a solvent instead of H_2O provides better contrast in neutron experiments. In SAXS experiments, however, the choice of solvent D_2O or H_2O does not matter.

3. Small-angle scattering analysis

The experimental details and the data analysis methods used for the two small-angle scattering techniques (SANS and SAXS) are similar and the only difference arises from characteristics of the radiation used. The difference in the interaction of neutrons and x-rays with matter gives rise to the different contrasts for the radiation. In a small-angle scattering experiment, one measures the differential scattering cross-section per unit volume ($d\Sigma/d\Omega$) as a function of the scattering vector Q ($=4\pi \sin\theta/\lambda$, where 2θ is the scattering angle and λ is the wavelength of

incident radiation), and for a micellar solution it can be expressed as [19]

$$\frac{\mathrm{d}\Sigma}{\mathrm{d}\Omega}(Q) = n[\langle F(Q)^2\rangle + \langle F(Q)\rangle^2(S(Q)-1)] + B \tag{1}$$

where n is the number density of the particles. $F(Q)$ is the single-particle form factor and depends on the shape and size of the particles. $S(Q)$ is the interparticle structure factor and is decided by the spatial distribution of the particles. B is a constant term that represents the incoherent scattering background, which occurs in the case of neutrons mainly due to hydrogen in the sample.

The micelles formed at the critical micelle concentration are spherical. If the solution conditions (e.g. concentration, ionic strength etc) of the micellar solutions are changed that favours the growth of the micelles; they grow along one of the axial directions of the micelles. The growth of the micelles as polydispersed spheres or along the other two axial directions is restricted by the maximum length of the surfactant molecule, to avoid energetically unfavourable empty space or water penetration inside the micelle [1, 2]. The prolate ellipsoidal shape ($a \neq b = c$) of the micelles is widely used in the analysis of small-angle scattering data because it also represents other different possible shapes of the micelles such as spherical ($a = b$) and rod-like ($a \gg b$). For such an ellipsoidal micelle

$$\langle F^2(Q)\rangle = \int_0^1 [F(Q,\mu)]^2\,\mathrm{d}\mu \tag{2}$$

$$\langle F(Q)\rangle^2 = \left[\int_0^1 F(Q,\mu)\,\mathrm{d}\mu\right]^2 \tag{3}$$

$$F(Q,\mu) = (\rho_\mathrm{m}-\rho_\mathrm{shell})V_\mathrm{m}\left[\frac{3j_1(x_m)}{x_m}\right] + (\rho_\mathrm{shell}-\rho_\mathrm{s})V_\mathrm{t}\left[\frac{3j_1(x_t)}{x_t}\right] \tag{4}$$

$$j_1(x) = \frac{(\sin x - x\cos x)}{x^2} \tag{5}$$

$$x_m = Q[a^2\mu^2 + b^2(1-\mu^2)]^{1/2} \tag{6}$$

$$x_t = Q[(a+t)^2\mu^2 + (b+t)^2(1-\mu^2)]^{1/2} \tag{7}$$

where ρ_m, ρ_shell and ρ_s are, respectively, the scattering length densities of the micelle, counterion shell and solvent. The dimensions a and b are, respectively, the semimajor and semiminor axes of the ellipsoidal micelle and t is the thickness of the shell of condensed counterions on the micelle. V_m ($=4\pi ab^2/3$) and V_t ($=4\pi(a+t)(b+t)^2/3$) are the volumes of the micelle and total volume of micelle along with the shell, respectively. The variable μ is the cosine of the angle between the directions of a and the wavevector transfer Q.

The expression for $S(Q)$ depends on the relative positions of the particles. In the case of an isotropic system, $S(Q)$ can be written as

$$S(Q) = 1 + 4\pi n\int (g(r)-1)\frac{\sin Qr}{Qr}r^2\,\mathrm{d}r \tag{8}$$

where $g(r)$ is the radial distribution function. $g(r)$ is the probability of finding another particle at a distance r from a reference particle centred at the origin. The details of $g(r)$ depend on the interaction potential $U(r)$ between the particles. For the results reported herein, $S(Q)$ has been calculated using the mean spherical approximation as developed by Hayter and Penfold [20]. The micelle is assumed to be a rigid equivalent sphere of diameter $\sigma = 2(ab^2)^{1/3}$ interacting through a screened Coulomb potential, which is given by

$$u(r) = u_0\sigma\frac{\exp[-\kappa(r-\sigma)]}{r}, \qquad r > \sigma \tag{9}$$

where κ is the Debye–Hückel inverse screening length and is calculated as

$$\kappa = \left[\frac{8\pi N_A e^2 I}{10^3 \varepsilon k_B T}\right]^{1/2} \tag{10}$$

defined by the ionic strength I of the solution

$$I = \mathrm{CMC} + \tfrac{1}{2}\alpha C + C_s. \tag{11}$$

I is determined by the CMC, dissociated counterions from the micelles and the salt concentration. The fractional charge α ($=Z/N$, where Z is the micellar charge) is the charge per surfactant molecule in the micelle and is a measure of the dissociation of the counterions of the surfactant in the micelle. C and C_s present the concentrations of the surfactant and salt in the solution, respectively. The contact potential u_0 is given by

$$u_0 = \frac{Z^2 e^2}{\pi \varepsilon \varepsilon_0 \sigma (2 + \kappa\sigma)^2} \tag{12}$$

where ε is the dielectric constant of the solvent medium, ε_0 is the permittivity of free space and e is the electronic charge.

The dimensions of the micelle, aggregation number and the fractional charge have been determined from the analysis. The semimajor axis (a), semiminor axis ($b = c$) and the fractional charge (α) are the parameters used in analysing the SANS data. The aggregation number is calculated using the relation $N = 4\pi ab^2/3v$, where v is the volume of the surfactant monomer. The above structure and interaction information about the micelles as obtained from SANS is used to fit the SAXS data and the thickness of the condensed counterions around the micelle (t) is obtained as an additional parameter. The scattering from the dissociated counterions is neglected due to their small volume and low number fraction. The parameters in the analysis were optimized by means of a nonlinear least-squares fitting program [21].

4. Results and discussion

Figure 1 shows the SANS data on the 100 mM CTABr micellar solution and in the presence of a varying concentration of KCl. The inset shows the variation of the neutron scattering length densities for different components of the micelles in 100 mM CTABr micellar solution. The contrast for any component depends on the square of the difference of the scattering length densities of that component and the solvent. It is clear from the variation of the scattering length density for neutrons that there exists a very strong contrast for the micelles in D_2O with respect to that for the counterions. This makes the scattering from counterions negligible and neutrons only 'see' the core of the micelles. All the SANS data show a correlation peak, which is due to peak from the interparticle structure factor $S(Q)$ [9, 10]. The peak usually occurs at $Q_m \sim 2\pi/d$, where d is the average distance between the micelles and Q_m is the value of Q at the peak position. The correlation peak broadens without any significant shift in the peak position. The screening in the presence of salt reduces the extent of the short-range order between the charged micelles, which, in turn, broadens the peak. The micellar size and interaction parameters in these systems are given in table 1. It is seen that fractional charge α on the micelle decreases and the aggregation number increases when the electrolyte concentration in the micellar solution is increased. This suggests an increase in counterion condensation $(1 - \alpha)$ on the micelle as the electrolyte is added. The charge neutralization at the surface of the micelle caused by the increase in the counterion condensation decreases the effective head group area for the surfactant monomer to occupy in the micelle and hence the increase in the aggregation number of the micelle occurs. It may be mentioned that although counterions

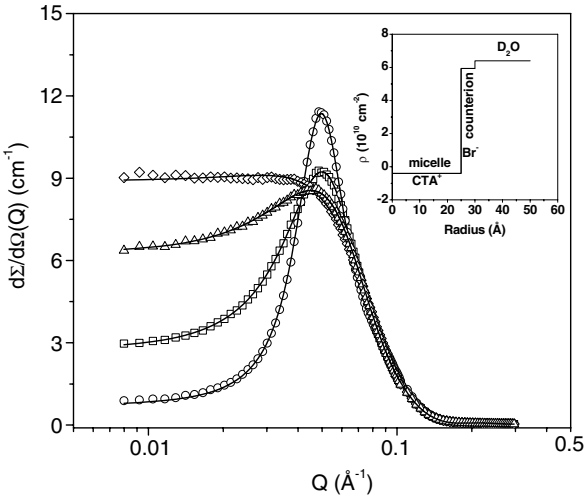

Figure 1. SANS data from a micellar solution of 100 mM CTABr in the presence of varying KCl concentrations. The data from bottom to top in the low Q region correspond to the KCl concentrations of 0, 20, 60 and 100 mM. The inset shows the variation of the neutron scattering length density for different components of the micelle in 100 mM CTABr micellar solution.

Table 1. Micellar parameters as obtained by SANS for 100 mM CTABr in the presence of a varying concentration of KCl.

Micellar system	Aggregation number N	Semiminor axis $b = c$ (Å)	Semimajor axis a (Å)	Fractional charge α	Counterion condensation $1 - \alpha$ (%)
100 mM CTABr	174 ± 9	24.0 ± 0.5	40.2 ± 1.2	0.23 ± 0.01	77
100 mM CTABr + 20 mM KCl	189 ± 9	24.6 ± 0.5	41.8 ± 1.2	0.19 ± 0.01	81
100 mM CTABr + 60 mM KCl	202 ± 10	24.6 ± 0.5	44.7 ± 1.2	0.16 ± 0.01	84
100 mM CTABr + 100 mM KCl	208 ± 11	24.6 ± 0.5	46.0 ± 1.2	0.11 ± 0.01	89

for micellar solution prepared in H_2O will give a very good contrast ($(\rho_{shell} - \rho_s)^2$), the large incoherent scattering background from H_2O as the solvent as compared to the low scattering from counterions makes it difficult to separate the scattering contribution of the condensed counterions.

Figure 2 shows the SAXS data corresponding to the same samples for which the SANS data are shown in figure 1. The inset shows the variation of the x-ray scattering length densities for different components of the micelles in 100 mM CTABr micellar solution. Unlike in the case of neutrons, it is seen that for x-rays there exists a similar contrast for counterions and the core of the micelles. SAXS data similarly to SANS data show correlation peaks, at the same Q values. The fact that the average distance between the micelles mainly decides the position of the correlation peak is independent of the radiation used. The second peak in the SAXS data at higher Q values arises from scattering of shell-like structure of the condensed counterions around the micelles [14–16]. In principle, it is possible to use contrast variation in SANS by mixing H_2O and D_2O to get information similar to that obtained using SAXS. However, this method does not work for the present system due to very small scattering of neutrons from counterions. The total volume fraction of counterions in the shell of condensed counterions is only about 10%. As a result, the contrast is dominated by the hydration in the

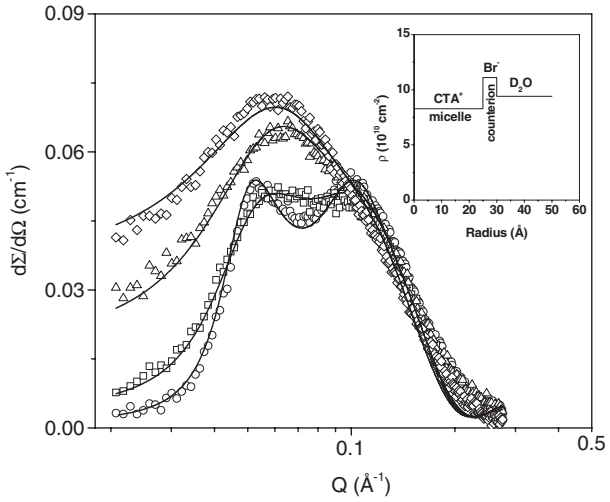

Figure 2. SAXS data from a micellar solution of 100 mM CTABr in the presence of varying KCl concentrations. The data from bottom to top in the low Q region correspond to the KCl concentrations of 0, 20, 60 and 100 mM. The inset shows the variation of the x-ray scattering length density for different components of the micelle in 100 mM CTABr micellar solution.

Table 2. Micellar parameters as obtained from SAXS for 100 mM CTABr in the presence of a varying concentration of KCl.

Micellar system	Number fraction of condensed Br^- counterions	Number fraction of condensed Cl^- counterions	Condensed counterions thickness, t (Å)
100 mM CTABr	1.0	0.0	4.2 ± 0.2
100 mM CTABr + 20 mM KCl	0.83	0.17	4.3 ± 0.2
100 mM CTABr + 60 mM KCl	0.63	0.37	4.4 ± 0.2
100 mM CTABr + 100 mM KCl	0.5	0.5	4.5 ± 0.2

shell. Also minimizing the scattering from the core of the micelles needs a higher percentage of H_2O in H_2O and D_2O mixing, which will increase the neutron incoherent background significantly.

The changes in features of SAXS data with the addition of KCl in CTABr micellar solution are significantly different to those for SANS data. The two-peak characteristics of SAXS data in pure CTABr micellar solution gradually change to one-peak data with the addition of electrolyte. This is an indication that the scattering from the condensed counterions decreases with the addition of electrolyte. This is possible if some of the Br^- (higher atomic number) counterions are exchanged with the added Cl^- (lower atomic number) counterions. In fact, the same is confirmed by the detailed analysis of the SAXS data. The data could only be fitted when the exchange of counterions (Br^- for Cl^- counterions) for the condensed counterions is considered. The amount of exchanged counterions is decided by the diffusion process, which at equilibrium maintains the same concentration gradient $((C_t - C_{cond})/C_t$, where C_t and C_{cond} are the concentrations of the total and condensed counterions in the micellar solution, respectively) for each of the counterions. The calculated curves for $\langle F^2(Q)\rangle$, $S(Q)$ and $d\Sigma/d\Omega(Q)$ of the SANS (figure 1) and SAXS (figure 2) data are shown in figures 3 and 4, respectively. Table 2 shows the fitted number fraction of the condensed Br^- and Cl^- counterions around the micelle along with the thickness of shell over which they are condensed. The distribution of

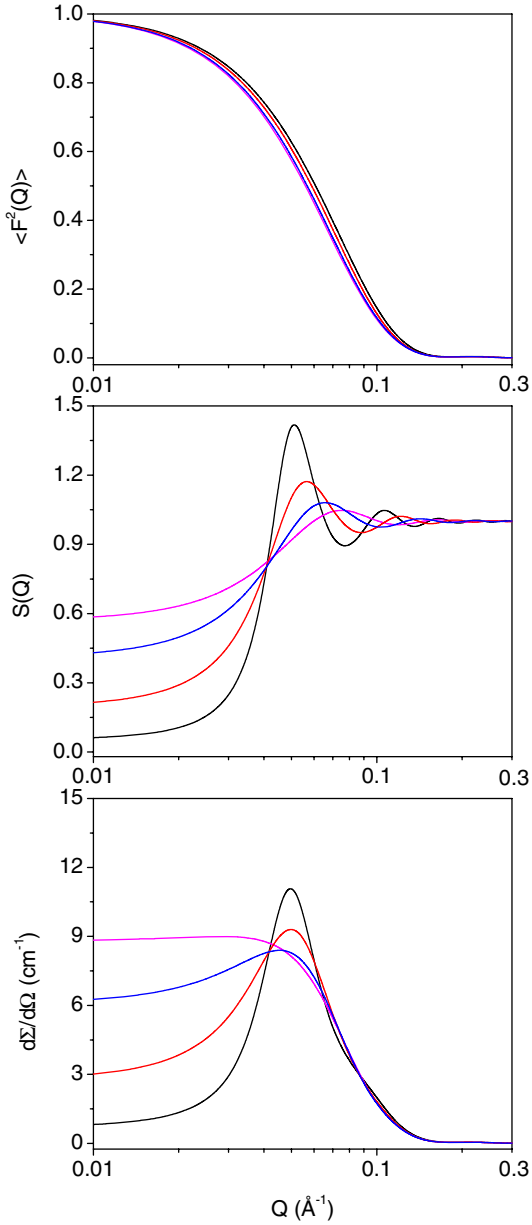

Figure 3. Fitted curves for $\langle F^2(Q)\rangle$, $S(Q)$ and $\mathrm{d}\Sigma/\mathrm{d}\Omega(Q)$ for SANS data from 100 mM CTABr in the presence of 0, 20, 60 and 100 mM KCl. $\langle F^2(Q)\rangle$ is normalized to unity at $Q = 0$ and the different distributions correspond to the decrease in the width of the distribution with increase in the KCl concentration. The different distributions both for $S(Q)$ and $\mathrm{d}\Sigma/\mathrm{d}\Omega(Q)$ from bottom to top correspond to increasing concentration of KCl.

condensed counterions is treated as a step function and it fits the data reasonably well perhaps due to the large condensation of the counterion on the charged micelles (table 1). It is found that the number fraction of condensed Cl^- counterions increases and that of Br^- counterions decreases with increase in the concentration of KCl. The thickness of the condensed shell

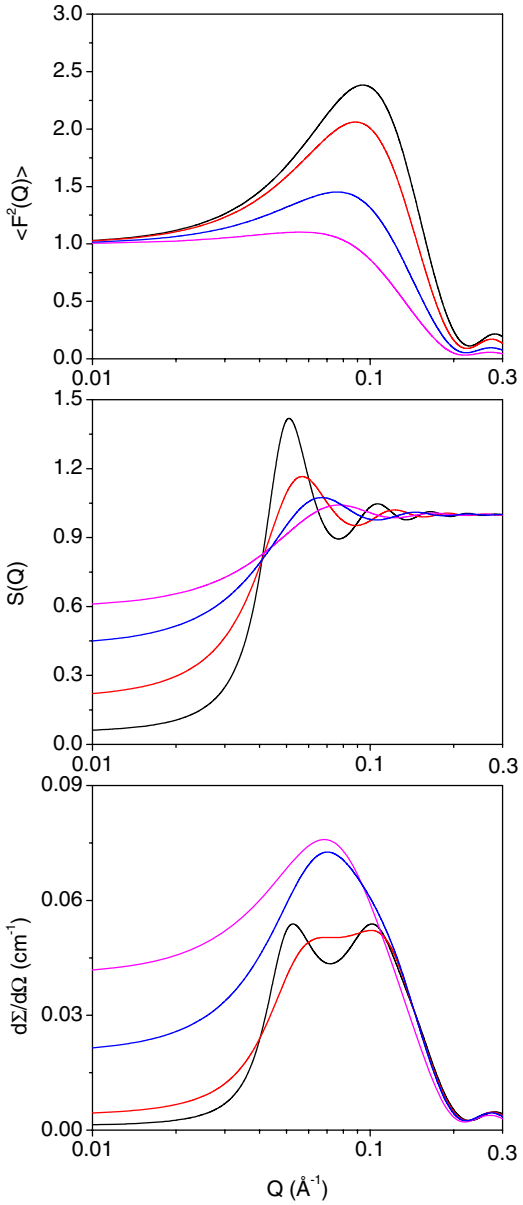

Figure 4. Fitted curves for $\langle F^2(Q)\rangle$, $S(Q)$ and $\mathrm{d}\Sigma/\mathrm{d}\Omega(Q)$ for SAXS data from 100 mM CTABr in the presence of 0, 20, 60 and 100 mM KCl. $\langle F^2(Q)\rangle$ is normalized to unity at $Q = 0$ and the different distributions correspond to the fall of the distribution with increase in the KCl concentration. The different distributions both for $S(Q)$ and $\mathrm{d}\Sigma/\mathrm{d}\Omega(Q)$ from bottom to top correspond to increasing concentration of KCl.

shows a trend of small increase with the addition of KCl as expected because of the exchange of Br^- counterions for Cl^- counterions. Usually, small ions are hydrated more and need larger thickness to condense on the micelles.

Figures 5 and 6, respectively, show SANS and SAXS data for 100 mM CTACl in the presence of varying concentrations of KBr. It is observed that unlike those for the CTABr/KCl

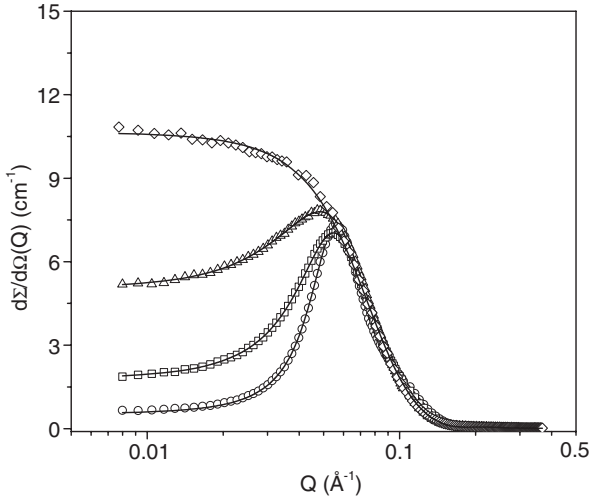

Figure 5. SANS data from a micellar solution of 100 mM CTACl in the presence of varying KBr concentrations. The data from bottom to top in the low Q region correspond to the KBr concentrations of 0, 20, 60 and 100 mM.

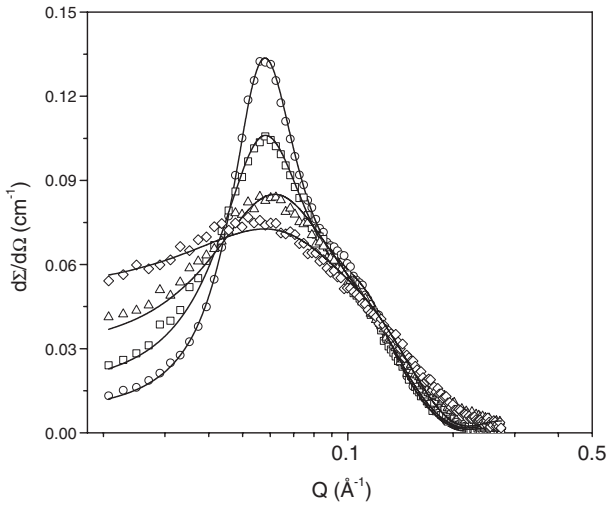

Figure 6. SAXS data from a micellar solution of 100 mM CTACl in the presence of varying KBr concentrations. The data from bottom to top in the low Q region correspond to the KBr concentrations of 0, 20, 60 and 100 mM.

micellar solutions, SANS data for CTACl/KBr on increasing the KBr concentration show an increase in the cross-section with a significant shift in the peak position towards the low Q region. This indicates the relatively large increase in the size of micelles on addition of KBr in CTACl compared with that for the addition of KCl in CTABr. Table 3 shows the micellar parameters for CTACl/KBr micellar solution with increasing concentration of KBr. It is seen that while the counterion condensation increases by about 30% with the addition of 100 mM KBr in CTACl micelles, the increase is about 15% with the addition of KCl in CTABr micelles.

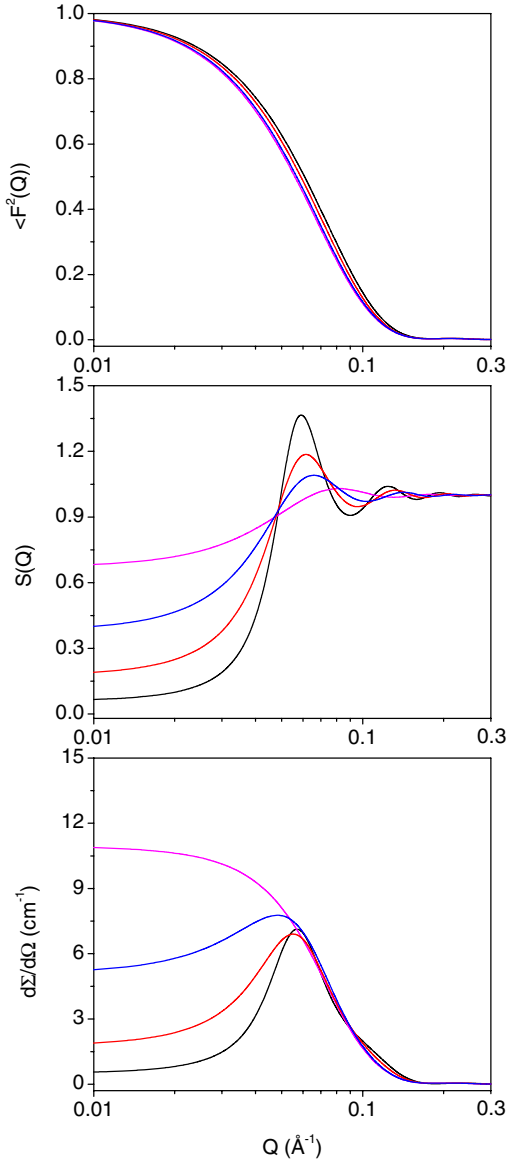

Figure 7. Fitted curves for $\langle F^2(Q)\rangle$, $S(Q)$ and $\mathrm{d}\Sigma/\mathrm{d}\Omega(Q)$ for SANS data from 100 mM CTACl in the presence of 0, 20, 60 and 100 mM KBr. $\langle F^2(Q)\rangle$ is normalized to unity at $Q = 0$ and the different distributions correspond to the decrease in the width of the distribution with increase in the KBr concentration. The different distributions both for $S(Q)$ and $\mathrm{d}\Sigma/\mathrm{d}\Omega(Q)$ from bottom to top correspond to increasing concentration of KBr.

That is, counterion condensation is more effective with the presence of Br^- counterions than with the presence of Cl^- counterions. The variation in scattering intensity for SAXS data for CTACl/KBr shows the opposite trend to that for CTABr/KCl. The cross-section decreases along with the broadening of the data with increasing KBr concentration. This again suggests a change of the contrast of the shell of counterions, which means that the Br^- counterions are exchanged with the condensed Cl^- counterions. The calculated curves for $\langle F^2(Q)\rangle$, $S(Q)$

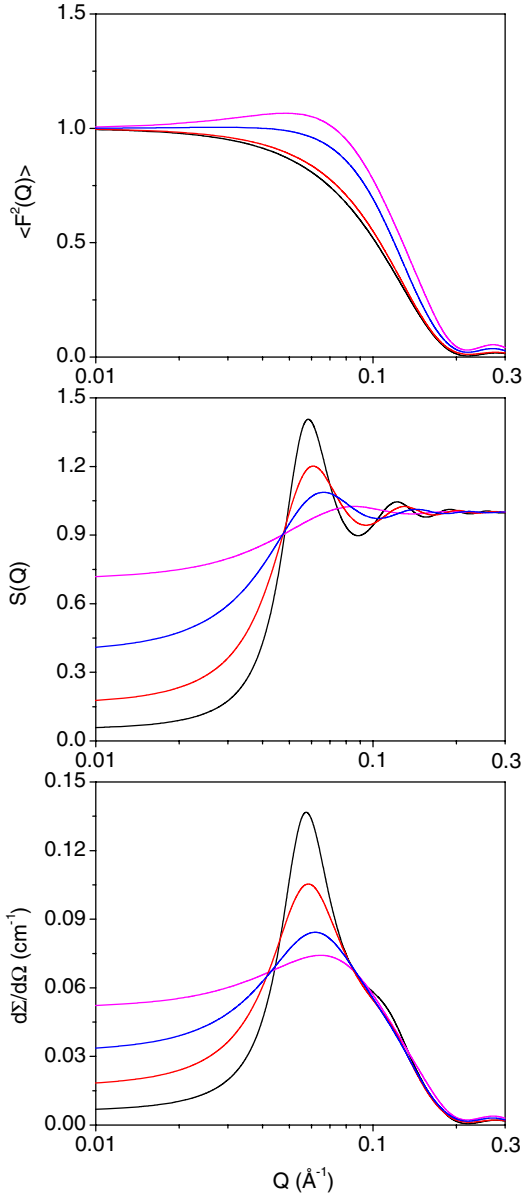

Figure 8. Fitted curves for $\langle F^2(Q)\rangle$, $S(Q)$ and $\mathrm{d}\Sigma/\mathrm{d}\Omega(Q)$ for SAXS data from 100 mM CTACl in the presence of 0, 20, 60 and 100 mM KBr. $\langle F^2(Q)\rangle$ is normalized to unity at $Q = 0$ and the different distributions correspond to a rise of the distribution with increase in the KBr concentration. The different distributions both for $S(Q)$ and $\mathrm{d}\Sigma/\mathrm{d}\Omega(Q)$ from bottom to top correspond to increasing concentration of KBr.

and $\mathrm{d}\Sigma/\mathrm{d}\Omega(Q)$ for the SANS (figure 5) and SAXS (figure 6) data for CTACl/KBr systems are shown in figures 7 and 8, respectively. Table 4 shows the fitted number fraction of the counterions that are condensed on the charged micelles. The thickness of the shell of condensed counterions shows a decreasing trend with increasing KBr as more and more Cl^- counterions are replaced by Br^- counterions.

Table 3. Micellar parameters as obtained from SANS for 100 mM CTACl in the presence of a varying concentration of KBr.

Micellar system	Aggregation number N	Semiminor axis $b = c$ (Å)	Semimajor axis a (Å)	Fractional charge α	Counterion condensation $1 - \alpha$ (%)
100 mM CTACl	116 ± 6	23.0 ± 0.5	29.1 ± 1.0	0.28 ± 0.01	72
100 mM CTACl + 20 mM KBr	140 ± 7	23.4 ± 0.5	34.2 ± 1.0	0.24 ± 0.01	76
100 mM CTACl + 60 mM KBr	187 ± 9	24.6 ± 0.5	41.3 ± 1.2	0.19 ± 0.01	81
100 mM CTACl + 100 mM KBr	228 ± 12	24.6 ± 0.5	50.4 ± 1.6	0.06 ± 0.02	94

Table 4. Micellar parameters as obtained from SAXS for 100 mM CTACl in the presence of a varying concentration of KBr.

Micellar system	Number fraction of condensed Br^- counterions	Number fraction of condensed Cl^- counterions	Condensed counterions thickness t, (Å)
100 mM CTACl	0.0	1.0	4.6 ± 0.2
100 mM CTACl + 20 mM KBr	0.17	0.83	4.6 ± 0.2
100 mM CTACl + 60 mM KBr	0.37	0.63	4.5 ± 0.2
100 mM CTACl + 100 mM KBr	0.5	0.5	4.4 ± 0.2

5. Conclusions

A combined use of SANS and SAXS has been made to achieve the direct observation of counterion condensation on charged micelles in aqueous electrolyte solution. It is found that the difference in condensation of Br^- and Cl^- counterions around the micelles gives rise to the different structures of CTABr and CTACl micelles. The addition of electrolytes KCl and KBr in CTABr and CTACl micellar solutions, respectively, shows exchange of the counterions to the extent that the concentration gradients of both the counterions (Br^- and Cl^-) around the charged micelles with respect to the solution remain the same.

References

[1] Degiorgio V and Corti M 1985 *Physics of Amphiphiles: Micelles, Vesicles and Microemulsion* (Amsterdam: North-Holland)
[2] Chevalier Y and Zemb T 1990 *Rep. Prog. Phys.* **53** 279
[3] Oosawa F 1971 *Polyelectrolytes* (New York: Dekker)
[4] Manning G S 1969 *J. Chem. Phys.* **51** 924
[5] Alexander S, Chaikin P M, Grant P, Morales G J, Pincus P and Hone D 1984 *J. Chem. Phys.* **80** 5776
[6] Ramanathan G V 1988 *J. Chem. Phys.* **88** 3887
[7] Belloni L 1998 *Colloids Surf.* A **140** 227
[8] Konop A J and Colby R H 1999 *Langmuir* **15** 58
[9] Aswal V K and Goyal P S 2000 *Phys. Rev.* E **61** 2947
[10] Aswal V K and Goyal P S 2002 *Chem. Phys. Lett.* **364** 44
[11] Borisov O V and Zhulina E V 2002 *Macromolecules* **35** 4472
[12] Allen R J and Warren P B 2003 *Europhys. Lett.* **64** 468
[13] Aswal V K and Goyal P S 2004 *PRAMANA—J. Phys.* **63** 65
[14] Wu C F, Chen S H, Shih L B and Lin J S 1988 *Phys. Rev. Lett.* **61** 645
[15] Aswal V K, Goyal P S, De S, Bhattacharya S, Amenitsch H and Bernstorff S 2000 *Chem. Phys. Lett.* **329** 336
[16] Vass S, Plestil J, Laggner P, Gilanyi T, Borbely S, Kriechbaum M, Jakli G, Decsy Z and Abuja P M 2003 *J. Phys. Chem.* B **107** 12752
[17] Kohlbrecher J and Wagner W 2000 *J. Appl. Crystallogr.* **33** 804
[18] Amenitsch H, Bernstorff S, Kriechbaum M, Lombardo D, Mio H, Rappolt M and Laggner P 1997 *J. Appl. Crystallogr.* **30** 872
[19] Chen S H and Lin T L 1987 *Methods of Experimental Physics* vol 23B, ed D L Price and K Skold (New York: Academic) p 489
[20] Hayter J B and Penfold J 1981 *Mol. Phys.* **42** 109
[21] Bevington P R 1969 *Data Reduction and Error Analysis for Physical Sciences* (New York: McGraw-Hill)